Analysis of sampled fiber Bragg gratings in polarization-maintaining fiber

Yongqing Lei (雷永庆), Jue Wei (韦 珏), Xiaofeng Xu (徐晓峰), and Yajuan Li (李亚娟)

Key Laboratory of Coherent Light, Atomic and Molecular Spectroscopy,
College of Physics, Jilin University, Changchun 130023

Received December 13, 2007

A novel type of sampled fiber Bragg gratings (FBGs) written in polarization-maintaining fiber (PMF) is proposed. The reflection spectrum, time delay, and group velocity dispersion (GVD) of the gratings are analyzed. In addition, the reflection spectrum is optimized by apodization. The scheme of multi-wavelength output based on the gratings is proposed, which could be used as a multi-wavelength polarization filter in the density wavelength division multiplexed (DWDM) system.

OCIS codes: 060.0060, 060.2280.
doi: 10.3788/COL20080607.0479.

The sampled fiber Bragg gratings (sampled FBGs), due to their unique advantages of multi-wavelength output, could be used to realize the multi-wavelength filter function[1−3]. To realize narrower channel spacing and expanding bandwidth under the premise of keeping flat output of channels with common sampled FBGs, people try to adjust the parameters such as sampling rate (SR), sampling period, and the length of the gratings. However, there is no obvious improvement. In the paper, the sampled FBGs written in polarization-maintaining fiber (PMF) are proposed. Due to the intrinsic birefringence of the fiber, each mode splits into two orthogonal linear polarization modes. This means the spectral response of the sampled FBGs written in PMF consists of two combs corresponding to orthogonal linear polarizations, and the spectral interval (Bragg central wavelength interval) between the combs could be changed by varying the fiber birefringence (difference of effective refractive indexes of fast-axis and slow-axis). By selecting suitable design parameters of the gratings such as sampling period, sampling rate, gratings length, and difference of effective refractive indexes, the gratings could be used as multi-wavelength polarization filters. To fully grasp the new type of gratings, time delay and group velocity dispersion (GVD) are also analyzed, which could affect the gratings' filtering capability. Due to great deal of side-lobe in the reflection spectrum of the gratings, to increase side mode suppression ratio (SMSR), the reflection spectrum could be optimized by apodization.

The fields of input port and output port of sampled FBGs are described by

$$\begin{pmatrix} A^{\mathrm{f}}(0) \\ A^{\mathrm{b}}(0) \end{pmatrix} = \vec{T} \begin{pmatrix} A^{\mathrm{f}}(L) \\ A^{\mathrm{b}}(L) \end{pmatrix} \begin{pmatrix} T_{11} & T_{12} \\ T_{21} & T_{22} \end{pmatrix} \begin{pmatrix} A^{\mathrm{f}}(L) \\ A^{\mathrm{b}}(L) \end{pmatrix}, \tag{1}$$

where A^{f} and A^{b} are the amplitudes of the forward and backward propagating fields respectively, L is the length of gratings, $T = T_1 T_2 \cdots T_i \cdots T_{m-1} T_m$ is the transfer matrix. When i is an odd number, T_i represents gratings segment, and when i is an even number, T_i represents the phase shift segment. According to the boundary condition: $A^{\mathrm{b}}(L) = 0$, the reflection coefficient r and the reflectivity R may be obtained as

$$r = A^{\mathrm{b}}(0)/A^{\mathrm{f}}(0) = T_{21}/T_{11}, \tag{2}$$

$$R = |r|^2, \tag{3}$$

where T_{11} and T_{21} are the ultimate transmission matrix elements. The Bragg central wavelength is a key variable for the sampled FBGs, and the Bragg central wavelength could be written as

$$\lambda_{\mathrm{B}} = 2n_{\mathrm{eff}}\Lambda. \tag{4}$$

When the sampled FBGs are written in the PMF, the gratings could realize more multi-wavelength outputs. In this case, the two sets of polarized reflection spectrum could be aligned along the fast-axis and the slow-axis of birefringence fiber, respectively.

The related equation of the Bragg central wavelength interval $\Delta\lambda_{\mathrm{B}}$ and the difference of effective refractive indexes of fast-axis and slow-axis Δn_{eff} is given by

$$\Delta\lambda_{\mathrm{B}} = \lambda_{\mathrm{B}}^{\mathrm{s}} - \lambda_{\mathrm{B}}^{\mathrm{f}} = 2(n_{\mathrm{eff}}^{\mathrm{s}} - n_{\mathrm{eff}}^{\mathrm{f}})\Lambda = 2\Delta n_{\mathrm{eff}}\Lambda, \tag{5}$$

where $\lambda_{\mathrm{B}}^{\mathrm{f}}$ and $\lambda_{\mathrm{B}}^{\mathrm{s}}$ are the Bragg central wavelengths of fast-axis and slow-axis, respectively, $n_{\mathrm{eff}}^{\mathrm{f}}$ and $n_{\mathrm{eff}}^{\mathrm{s}}$ are the effective refractive indexes of fast-axis and slow-axis, respectively, $\Delta n_{\mathrm{eff}} = n_{\mathrm{eff}}^{\mathrm{s}} - n_{\mathrm{eff}}^{\mathrm{f}}$.

When the grating period Λ is fixed, the spectral interval between two sets of reflection peaks is only related to the Δn_{eff}. For gratings in low-birefringence (Low-Bi) fiber, the frequency spacing (corresponding to $\Delta\lambda_{\mathrm{B}}$) can be only a few gigahertz[4], and for gratings in high-birefringence (Hi-Bi) one, the frequency spacing could be up to several hundred gigahertz[5,6]. In this paper, the Δn_{eff} has an important impact on the reflection spectrum of the sampled FBGs written in PMF, and it is in the order of $10^{-3} - 10^{-6}$, which leads to interval of two Bragg central wavelength from sub-nanometer (shown in Fig. 1(a)) to nanometer (shown in Fig. 1(b)). We should know even though the birefringence of PMF could be induced by external stresses, its high precise control is still

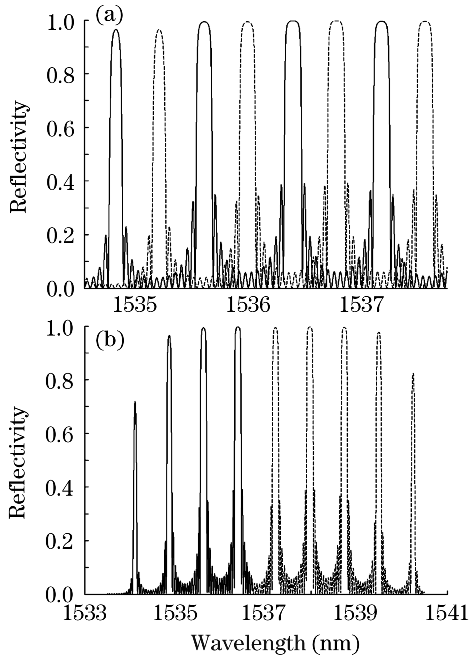

Fig. 1. Reflection spectrum of sampled FBGs in PMF, SR = 0.4. (a) $\Delta n_{\text{eff}} = 0.00035$, (b) $\Delta n_{\text{eff}} = 0.0035$. The solid curve and dotted curve depict the reflection spectrum of fast-axis and slow-axis, respectively.

very difficult. For current manufacturing technology level of PMF, high precise control of birefringence becomes the main obstacle.

Compared with the sampled FBGs written in conventional single mode fiber (SMF), a new type of gratings is used as a multi-wavelength filter, which has a narrower wavelength interval or more expanding bandwidth. We could use it to increase the number of channels which could expand communication capacity.

The GVD has already become an outstanding problem in the optical fiber communication system, therefore, the research of time delay and GVD of nonuniform fiber gratings has attracted considerable attentions[7]. For the optical pulse signal transmitted in the nonuniform fiber gratings, according to Eq. (2), the phase of reflection coefficient ψ, the time delay τ and GVD D could be gotten as follows:

$$\psi = \text{Arg}(r), \tag{6}$$

$$\tau = -\frac{\lambda^2}{2\pi c} \cdot \frac{\partial \psi}{\partial \lambda}, \tag{7}$$

$$D = \frac{\partial \tau}{\partial \lambda}, \tag{8}$$

where c is the light velocity in vacuum.

To analyze the time delay and GVD of the sampled FBGs written in PMF, we assume the sampled rate SR = 0.4, $\Delta n_{\text{eff}} = 0.0015$, and the numerical simulation result is shown in Fig. 2.

For the sampled FBGs in PMF, the central wavelength location of each channel not only has the maximal reflectivity (shown in Fig. 2(a)), but also has the linear time delay ripple (shown in Fig. 2(c)) and zero-dispersion (Fig. 2(d)). In addition, we find there is a larger GVD change at the location of band-gap edge and the side-lobe of the reflection spectrum. When the incidence wavelength meets the Bragg reflection condition, the gratings could play a stronger coupling role, on the contrary, the gratings have weaker coupling. So the gratings structure could be as Fabry-Perot cavity, and the zero reflectivity location of the gratings could be as the resonance peak location of Fabry-Perot cavity. These light waves at these wavelengths could be back and forth between gratings, therefore, they could have a larger time delay.

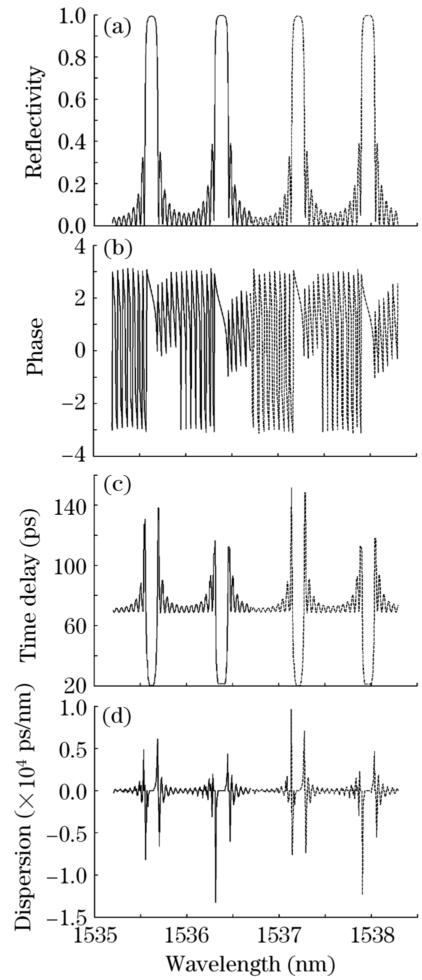

Fig. 2. Numerical simulation of sampled FBGs in PMF, SR = 0.4, $\Delta n_{\text{eff}} = 0.0015$. (a) Reflection spectrum; (b) phase ripple; (c) time delay ripple; (d) GVD ripple. The solid curve and dotted curve depict the reflection spectrum of fast-axis and slow-axis, respectively.

Due to the effect of Fabry Perot cavity resonance in the gratings, there is a great deal of side-lobe in the reflection spectrum of gratings. The reflection spectrum of sampled FBGs in conventional SMF has comb profile with narrower channel spacing, therefore, the side-lobe of each reflection peak could affect the neighboring one, and the crosstalk between the channels could be arisen from the side-lobe. The sampled FBGs in PMF not only have serious crosstalk of the sampled FBGs in conventional SMF, but also have the crosstalk between the channels of two orthogonal linear polarizations. While the nonuniform gratings are used in dense wavelength division multiplex (DWDM) system, the side-lobe could reduce the level of channel isolation, and the group delay ripple produces a signal that passes the gratings klirr and intersymbol interference, therefore, some measures should be adopted to suppress the crosstalk. The apodization of gradual change of refractive index modulation may achieve the purpose[8].

For the sampled FBGs in PMF, Super-Gauss function is an ideal apodization function. It means the effective refractive index distribution of the gratings is Super-Gaussian distribution, and the profile of reflection spectrum at each resonance wavelength is the same as the profile of Super-Gauss distribution. Using Super-Gauss function apodization, the effective refractive index variation can be expressed as

$$\overline{\delta n_{\mathrm{eff}}}(z) = \overline{\delta n_{\mathrm{eff}}} \exp(-G\frac{z^4}{\mathrm{FWHM}^4}), \quad \mathrm{FWHM} = a, \quad (9)$$

where $n_{\mathrm{eff}}(z)$ is the effective refractive index distribution along the z direction of gratings, FWHM is the full width at the half-maximum of Super-Gaussian distribution, a is the exposure region of gratings, G is the Gaussian factor. When G is 0, 10, 100, or 1000 respectively, the reflection spectrums with different Gaussian factors are shown in Fig. 3. When G is 0, it means no apodization. After the treatment of apodization, the side-lobe of reflection spectrum decreases obviously. From Fig. 3, we

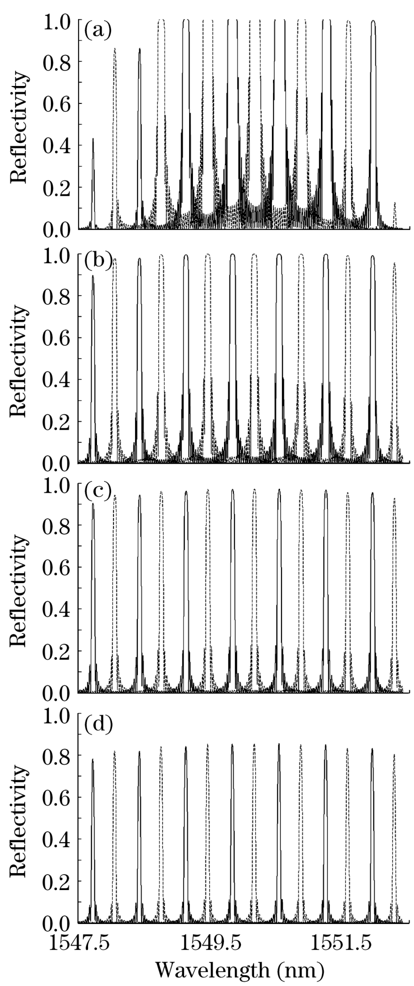

Fig. 3. SR = 0.42, (a) $G = 0$, (b) $G = 10$, (c) $G = 100$, (d) $G = 1000$. The solid curve and dotted curve depict the reflection spectrum of fast-axis and slow-axis, respectively.

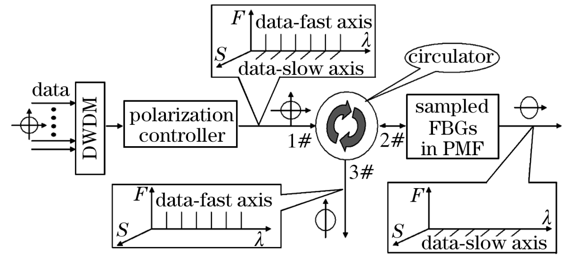

Fig. 4. Schematic of demultiplexer to be used when the incoming signals are orthogonally polarized.

know the numerical value of Gaussian factor is related to the channel power and flatness, so it is necessary to find a suitable Gaussian factor for optimization design of the filter.

The proposed new type of FBG could be used as a multi-wavelength polarization filter in polarization division multiplex (PDM) system. Polarization interleaving or multiplexing have been used in the quest to increase the spectral efficiency of DWDM optical transmission systems. PDM system could achieve double data output through transmitting two independently modulated and orthogonally polarized optical signals corresponding to the same frequency over a fiber[9,10]. The transmission line itself must meet two requirements for successful polarization division multiplexing/demultiplexing: 1) the overall difference in system gain for any two orthogonal polarizations must be less than a few decibels; 2) the overall time delay difference, between "fast" and "slow" polarizations, in the system for any two orthogonal polarizations must be small compared with a bit period. To demultiplex the signals at the receiving end, continuously adjustable polarization controller would be required, and could transform the data streams into two orthogonal linear polarizations[11]. The schematic of demultiplexer could be made as shown in Fig. 4.

The sampled FBGs in PMF could be used to realize polarization filtering function, whose reflection bandwidth is twice as much as the incoming signal bandwidths. The incoming signals (data of fast axis and slow axis) initially enter the 1# port of the circulator, and then they come out from 2# port and enter the sampled FBGs in PMF. Due to the Bagg reflection characteristic of the sampled FBGs in PMF, the signals (data of fast axis) corresponding to reflection wavelength of gratings could be reflected, and then be downloaded from 3# port. However, the remaining signals of the other polarization directions (data of low axis) are separated due to transmission.

In our application programs, where the overall gains for orthogonal polarizations would be substantially equal, the polarizations for the two channels would remain orthogonal throughout[11]. The transmission data is only related to single polarization state (fast axis or low axis), therefore, the sampled FBGs in PMF used in above two schemes cannot suffer from PMD problem.

A new type of sampled FBG in PMF is proposed. The reflection spectra, phase ripple, time delay ripple, and GVD ripple of the gratings are fully analyzed. A novel method to realize multi-wavelength output based on the sampled FBGs in PMF is proposed. The gratings have the advantages such as low dispersion, low cross talk, narrower channel spacing and more expanding bandwidth with flat multi-wavelength output. In addition, to realize ideal comb-filter, Supper-Gaussian apodization function is used to optimize the sampled FBGs in PMF. In a word, the new type of grating has a favorable application prospect in future.

X. Xu is the author to whom the correspondence should be addressed, his e-mail address is ccxuxiaofeng@yahoo.com.cn.

References

1. C. Wang, J. Azaña, and L. R. Chen, IEEE Photon. Technol. Lett. **16,** 1867 (2004).
2. J. E. McGeehan, M. C. Hauer, A. B. Sahin, and A. E. Willner, IEEE Photon. Technol. Lett. **15,** 1464 (2003).
3. M. Ibsen, M. K. Durkin, M. J. Cole, and R. I. Laming, IEEE Photon. Technol. Lett. **10,** 842 (1998).
4. M. Douay, T. Feng, P. Bemage, P. Niay, E. Delevaque, and T. Georges, IEEE Photon. Technol. Lett. **4,** 844 (1992).
5. D. Pureur, M. Douay, P. Bernage, P. Niay, and J. F. Bayon, J. Lightwave Technol. **13,** 350 (1995).
6. W. H. Loh, J. P. de Sandro, G. J. Cowle, B. N. Samson, and A. D. Ellis, Electron. Lett. **33,** 594 (1997).
7. J.-C. Dung and S. Chi, Opt. Commun. **162,** 219 (1999).
8. L. Wang, F. Yan, Y. Li, T. Gong, and S. Jian, Acta Opt. Sin. (in Chinese) **27,** 587 (2007).
9. P. M. Hill, R. Olshansky, and W. K. Burns, IEEE Photon. Technol. Lett. **4,** 500 (1992).
10. S. Hinz, D. Sandel, R. Noé, and F. Wüst, Electron. Lett. **36,** 1402 (2000).
11. S. G. Evangelides, Jr., L. F. Mollenauer, J. P. Gordon, and N. S. Bergano, IEEE J. Lightwave Technol. **10,** 28 (1992).